First publ. in: Thin Solid Films 496 (2006), pp. 417-419

Thermal stability of Fe/Mo layers

A. Liebig [a,*], B. Hjörvarsson [a], U. Rüdiger [b]

[a] *Department of Physics, Uppsala University, Box 530, S-75121 Uppsala, Sweden*
[b] *Fachbereich Physik, Universität Konstanz, D-78457 Konstanz, Germany*

Received 16 February 2005; received in revised form 2 August 2005; accepted 17 August 2005
Available online 28 September 2005

Abstract

The thermal stability of an iron/molybdenum bilayer was determined using Rutherford backscattering spectrometry and X-ray diffraction. Substantial interdiffusion (3%) was observed upon annealing at 973 K for one hour. High temperature annealing of Fe/Mo layers in oxygen ambient is therefore not suitable for the formation of magnetite layers.

Keywords: Interdiffusion; Thermal stability; X-ray diffraction; Spin polarisation

1. Introduction

The half-metallic Fe_3O_4 (magnetite) has attracted considerable interest, as it exhibits many of the properties required for successful realization of spintronic devices. Substantial work has therefore been invested on the growth of magnetite, with the goal to achieve maximum spin polarisation [1–5]. The growth has been performed by different techniques, for example reactive sputtering, plasma-assisted molecular beam epitaxy and oxidation of iron (110) surfaces.

High quality magnetite films can be obtained by high temperature oxidation of iron films [2,6]. This route is possible as the magnetite layers are almost perfectly lattice matched to the Fe layers and can therefore grow coherently without substantial defect generation in the oxide. Typically, a comparatively thick iron layer is grown and subsequently oxidised at temperatures around 970 K by oxygen exposures between 600 and 9000 Langmuir. The substrates used for the iron growth need therefore to fulfill two conditions: They have to have suitable lattice parameter for epitaxial growth of Fe, and have to be chemically stable, hindering interdiffusion during the oxidation step. For single monolayers, where the exposure to high temperatures is short, Pt(111) [7] is suitable, for thicker films and longer oxidation steps Mo(110) and W(110), either as single crystals [2] or as thin films on sapphire substrates [3,6], have been used.

The magnetite films prepared on molybdenum surfaces have previously been shown to exhibit significantly lower spin polarization, as compared to those prepared on tungsten substrates [3]. This is somehow surprising as the lattice parameter of Mo is closer to that of Fe. The structural quality of the Fe films is therefore expected to be better on Mo resulting in better quality of the magnetite layer. The most probable explanation to the reduced polarization is therefore the presence of uncompensated impurities in the Fe layers, which would require large interdiffusion of Mo in the Fe during the annealing process. This is supported by the binary phase diagram [8] which shows a Mo solubility of 3% in the α-Fe phase at 970 K. As a comparison, the solubility of W in Fe is below one percent at 1150 K, with extremely slow kinetics. Although the binary phase diagram supports the presence of Mo in Fe, the kinetics of the intermixing is unknown. Firm conclusion requires therefore direct measurements of the chemical stability of the Mo/Fe layers, which are presented on the following pages.

2. Experiment

The investigated films were grown by molecular beam epitaxy in an ultra high vacuum system, with a base pressure in the $3*10^{-8}$ Pa range. The substrates used were $Al_2O_3(11\bar{2}0)$

* Corresponding author. Fax: +46 18 4713524.
E-mail address: andreas.liebig@fysik.uu.se (A. Liebig).

single crystals (10×10 mm^2), cleaned in acetone and subsequently annealed in ultra high vacuum to 1073 K prior to deposition. The growth followed the recipe given in Ref. [9]. For details of growth see also Refs. [10,11].

The 15 nm thick molybdenum seed layers were deposited at 1073 K. After cooling to room temperature, the iron films (thickness 25 nm) were deposited, with a deposition rate of around 0.7 Å/s. After deposition, the samples were annealed to 773 K for one hour in order to improve the crystallinity. The surface quality was investigated after each step using Low Energy Electron Diffraction (LEED). Two reference samples were also grown, one annealed at 773 K as described above, and a second one without any heat treatment after deposition.

The surface composition of the Fe layers upon annealing was investigated using Auger Electron Spectroscopy (AES). The AES was performed on one sample by alternating measurement and annealing steps at 973 K for 1200 s in an attempt to follow the eventual Mo enrichment on the surface.

Rutherford backscattering spectrometry (RBS) was used to determine the film composition. The RBS (ex situ) was performed with single charged He^+ ions at a primary beam energy of 2.00 MeV, at a scattering angle of 160°. The measurements were performed at different tilt angles, to avoid accidental channeling. The Rump software package from CGS [12], utilizing the algorithm described by Doolittle [13], was used for the analysis of the RBS data.

X-ray diffractometry (XRD) was used to determine the out-of-plane lattice parameter as well as the coherence length of the layers. The X-ray analysis was performed in a Bragg–Brentano geometry, using a commercial Siemens D 5000 diffractometer with Cu Kα radiation.

3. Results and discussion

Annealing to 773 K developed clearly the rectangular LEED pattern of the Fe(110) surface as shown in Fig. 1. No changes were observed in the LEED pattern after the subsequent annealing steps. Since the LEED solely reflects the surface structure, XRD was used to investigate the crystalline quality of the films. The out-of-plane coherence length of the layers was determined from the full width at half maximum of the Mo and Fe peaks, using the Scherrer formula [14]. The resulting coherence lengths correspond to the thickness of the layers, hence, the quality is as good as it can be with respect to the out of plane coherency.

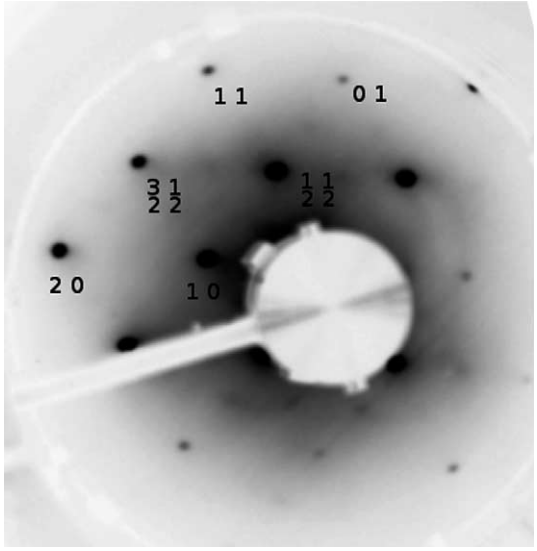

Fig. 1. LEED image of the Fe(110) surface. Sample slightly tilted with respect to the primary beam, electron energy 205 eV.

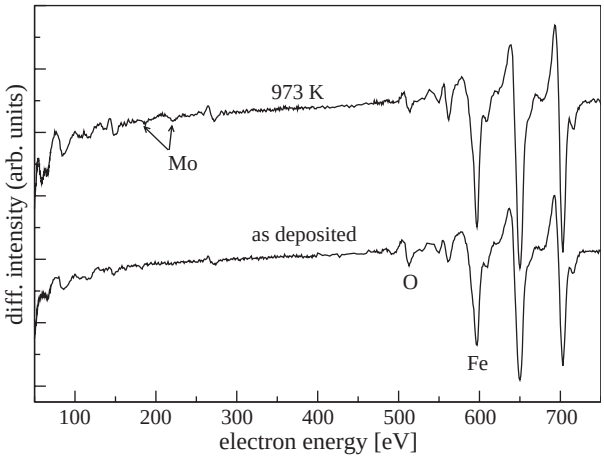

Fig. 2. Auger electron spectra, 3 keV primary energy, normal incidence, before and after annealing.

The change in the surface concentration of molybdenum upon annealing was determined using AES. No sign of Mo was observed after the initial annealing to 773 K. After nine annealing steps to 973 K, corresponding to total annealing time of 3 h, the molybdenum MNN lines at 186 eV and 221 eV are still weak (see Fig. 2). Hence, only a low Mo concentration (≈1 at.%) is found at the Fe surface, even after long annealing times. However, even in case of equilibrium solution of Mo in Fe, the surface concentration would be still close to the detection limit of this setup. Thus, a large Mo signal requires preferential surface segregation of Mo.

The degree of interdiffusion can conveniently be determined using RBS. Fig. 3 shows the results from a sample after

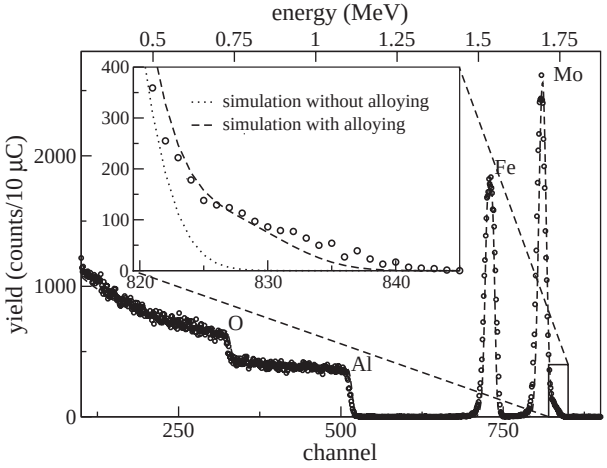

Fig. 3. RBS spectrum of annealed (973 K) sample. Open circles show measured points.

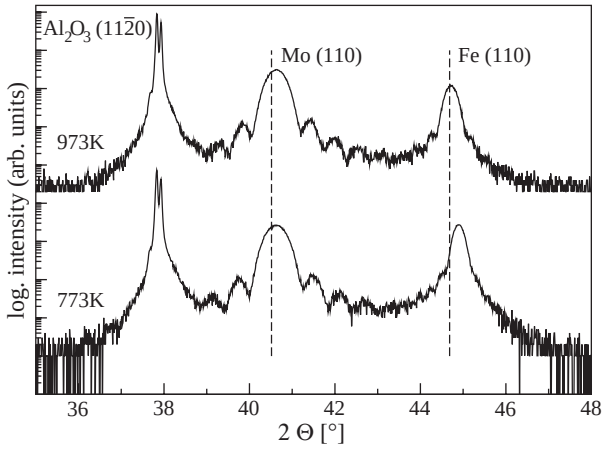

Fig. 4. X-ray diffraction patterns of samples annealed at different temperatures. The positions of the peaks for bulk Fe and Mo are marked.

annealing at 973 K for one hour. The signal from Mo and Fe, as well as the contribution from the substrate, is clearly separated. As seen in the figure, there is a significant shoulder at the Mo-high energy side (around 1.65 MeV), indicating the presence of Mo in the Fe layer. According to the simulations of the results, this contribution corresponds approximately to 3% of Mo in the Fe film. The results from the simulation are shown as an inset of the figure. Thickness variation of the Fe film, which could lead to similar RBS results, are not expected as the tailing is only seen in samples annealed at 973 K. Furthermore, the XRD results are inconsistent with large a thickness variation as seen by the coherence length as well as the presence of the well defined Kiessig fringes.

Further proof comes from the changes in the average lattice parameters of the layers upon annealing. If Mo (bcc, $a=0.315$ nm) is present in the Fe (bcc, $a=0.286$ nm) layers, it must influence the average lattice parameter of the Fe layer. With 3 at.% of Mo in the Fe layers, the shift should be measurable using standard XRD equipment as long as Vegard's law is fulfilled. On the other hand, if the tailing of the Mo towards higher energies in the RBS spectrum would be due to thickness variations of the Fe layer, the Fe(110) atomic plane distance should be unaffected.

Fig. 4 shows the diffraction pattern of two of the investigated samples. The dashed lines mark the peak positions for bulk Fe(110) and Mo(110). A substantial shift of the iron (110) peak is observed between the two samples. Annealing to 973 K shifts the diffraction peak to lower angles, d-value of 2.025 Å, corresponding to a lattice expansion of 0.3%. Applying Vegard's law, the shift yields an average alloying of 3% to 4% of molybdenum into the iron, which is completely in line with the RBS results and the solubility of Mo in Fe. Thus, we conclude that the annealing to 973 K results in complete formation of the alpha phase of Mo in Fe.

4. Conclusions

The results unambiguously prove the diffusion of Mo in Fe films during annealing steps, required for the formation of good crystalline magnetite films. As the presence of Mo significantly reduces the spin polarization [3] the results disqualify high temperature annealing (>970 K) of Mo/Fe layers as a step in the formation of highly spin-polarized magnetite films.

Acknowledgements

The Authors would like to thank C. Chacon for the help with the RBS measurements.

A. Liebig was supported during this work by a DAAD scholarship.

References

[1] W. Weiss, A. Barbieri, M.A. Van Hove, G.A. Somorjai, Phys. Rev. Lett. 71 (12) (1993) 1848.
[2] H.-J. Kim, J.-H. Park, E. Vescovo, Phys. Rev., B 61 (2000) 15284.
[3] M. Fonin, Y.S. Dedkov, J. Mayer, U. Rüdiger, G. Güntherodt, Phys. Rev., B 68 (2003) 045414.
[4] J.F. Bobo, D. Basso, E. Snoeck, C. Gatel, D. Hrabovsky, J.L. Gauffier, L. Ressier, R. Mamy, S. Visnovsky, J. Hamrle, J. Teillet, A.R. Fert, Eur. Phys. J., B Cond. Matter Phys. 24 (2001) 43.
[5] W. Kim, K. Kawaguchi, N. Koshizaki, M. Sohma, T. Matsumoto, J. Appl. Phys. 93 (10) (2003) 8032.
[6] Y. Dedkov, U. Rüdiger, G. Güntherodt, Phys. Rev., B 65 (2002) 064417.
[7] W. Weiss, G.A. Somorjai, J. Vac. Sci. Technol., A, Vac. Surf. Films 11 (4) (1993) 2138.
[8] Binary Alloy Phase Diagrams, second edition, ASM International, 1996.
[9] U. May, R. Calarco, J.O. Hauch, H. Kittur, M. Fonine, U. Rüdiger, G. Güntherodt, Surf. Sci. 489 (2001) 144.
[10] M. Tikhov, E. Bauer, Surf. Sci. 232 (1990) 73.
[11] J. Malzbender, M. Przybylsky, J. Giergel, J. Kirschner, Surf. Sci. 414 (1998) 187.
[12] M. Thompson, Rump–rbs analysis and simulation package (v 4.00(beta)), http://www.genplot.com, 2004.
[13] L.R. Doolittle, Nucl. Instrum. Methods Phys. Res., B Beam Interact. Mater. Atoms 15 (1985) 227.
[14] B.D. Cullity, Elements of X-Ray Diffraction, 2nd edition, Addison-Wesley Publishing Company, Inc., 1978, p. 102, Ch. 3.